RSC Advances

PAPER

View Article Online
View Journal | View Issue



Cite this: *RSC Adv.*, 2020, **10**, 2416

# Microwave-assisted synthesis of coal fly ash-based zeolites for removal of ammonium from urine

Boitumelo Makgabutlane,[ab] Lebea N. Nthunya,[c] Nicholas Musyoka,[d] Bongumusa S. Dladla,[e] Edward N. Nxumalo[a] and Sabelo D. Mhlanga *[ab]

Received 3rd December 2019
Accepted 26th December 2019

DOI: 10.1039/c9ra10114d

rsc.li/rsc-advances

Zeolites synthesized from biomass waste materials offer a great opportunity in the sustainable utilization of the waste. In this work, energy-efficient processes (*i.e.* microwave and ultrasound irradiation) were used to synthesize pure phase sodalite (zeolite) from coal fly ash obtained from a power plant in South Africa. The pure-phase sodalite was obtained with a comparatively higher surface area (16 $m^2 g^{-1}$) and cation exchange capacity (2.92 meq. $g^{-1}$) with 40 min total reaction time. The removal of ammonium from urine was carried out using (i) the coal fly ash-derived sodalite, (ii) raw coal fly ash and (iii) a commercially available natural zeolite (clinoptilolite). The pure phase sodalite exhibited the highest removal efficiency of about 82% and 73% in synthetic and real hydrolyzed urine respectively. The adsorption process followed the pseudo second-order kinetic model and the Freundlich adsorption isotherm, indicating that the adsorption process occurred on a heterogeneous surface.



## Introduction

Urine is the most nutrient-rich part of domestic wastewater, even though it constitutes only 1% of the total wastewater volume.[1] It contains essential nutrients such as nitrogen (N) in the form of ammonium ($NH_4^+$), phosphorus (P) and potassium (K) which can be recovered and used to make fertilizer.[2] If these nutrients are not recovered and find their way to the water bodies, they lead to eutrophication which is harmful to aquatic life.[3] In developing countries, where most communities do not have access to proper sanitation, waste disposal and management is a challenge. The waste is disposed into rivers that are often used for drinking purposes, rendering the water not safe for consumption and a major cause of waterborne diseases. However, the urine in the wastewater could be separated prior to discharge into water sources and converted to useful fertilizer for agricultural applicants. For instance, schools in the rural communities of South Africa and many other African countries use source separate toilets (especially male toilets) which would make urine collection for the recovery and recycling of nutrients possible.[2]

The recovery of K-struvite ($KMgPO_4 \cdot 6H_2O$) fertilizer from urine is of great interest because potassium is overlooked in the recovery of valuable nutrients even though it forms an essential part in NPK fertilizers.[4] The natural source of K (potash) is presumed to run out in the near decades, thus calling for alternative sources of K such as urine, to be explored. To recover K-struvite, nitrogen (N) in the form of the ammonium ($NH_4^+$) needs to be removed. This is because magnesium–ammonium–phosphate (MAP) also referred to as ammonium struvite ($NH_4MgPO_4 \cdot 6H_2O$) is readily formed during the precipitation process[5] and so it interferes with the magnesium–potassium–phosphate (MPP) precipitation. As such, the ammonium must be removed from urine, to favor the precipitation of K-struvite.

Conventional methods for the removal of ammonium from aqueous solutions have been studied using air stripping,[6] biological nitrification–denitrification[7] and ion-exchange.[8] Air stripping and ion exchange have been shown to be the technologies with the highest ammonia removal in urine (Table 1). The removal percentage is around 97% and these technologies can have higher ammonia removal even up to 100% with optimum conditions. Among the various methods, ion-exchange remains the most widely used due to its simplicity, environmental friendliness and low cost practicability.[9] Additionally, zeolites have been explored as low-cost materials for wastewater treatment. Clinoptilolite, among other natural zeolites, has demonstrated high cation exchange capacity and selectivity for the ammonium ion.[10] It has been used to treat water with high ammonium concentration such as greywater.[9]

[a]*Nanotechnology and Water Sustainability Research Unit, College of Science, Engineering and Technology, University of South Africa, Florida, 1709, Johannesburg, South Africa*

[b]*DST/MINTEK Nanotechnology Innovation Centre and SabiNano Pty Ltd, Mintek, 200 Malibongwe Drive, Strijdom Park, Randburg, 2194, Johannesburg, South Africa. E-mail: sdmhlanga1@gmail.com; smhlanga@sabinano.co.za*

[c]*Department of Chemical, Metallurgical and Material Engineering, Tshwane University of Technology, Private Bag X680, Pretoria, 0001, South Africa*

[d]*HySA Infrastructure Centre of Competence, Energy Centre, Council for Scientific and Industrial Research (CSIR), Meiring Naude Road, Brummeria, Pretoria, 0001, South Africa*

[e]*Department of Chemistry, College of Science, Engineering and Technology, University of South Africa, Florida, 1709, Johannesburg, South Africa*

Owing to their low-cost, high selectivity at low temperatures and environmental friendliness of releasing non-toxic exchangeable cations such as $Na^+$, $Ca^+$ and $Mg^+$, natural zeolites receive greater interest compared to synthetic cation exchange materials such organic resins.[11]

Zeolite materials occur either naturally or are synthesized from waste materials such as coal fly ash. Although coal fly ash is regarded as waste, it has a high content of valuable Si and Al and can be used as a precursor for the synthesis of zeolite.[19–22] Zeolites synthesized from coal fly ash have shown high cation exchange capacity and selectivity compared to natural zeolites.[23,24] As a result, they have gained more attention as adsorbents and catalysts in water treatment. Most studies on the synthesis of zeolites from coal fly ash have reported the use of fusion and hydrothermal methods which are energy intensive,[25–28] hence they are not environmentally friendly nor economically viable.

Microwave and ultrasound energies provide a viable alternative for zeolite synthesis since these methods consume less energy and reduce the reaction time. Microwave irradiation increases the rate of a chemical reaction and gives a rapid homogeneous heating of the reaction solution, leading to a more abundant nucleation.[20] The mechanism of energy transfer due to microwave irradiation and ultrasound irradiation is different from that of conventional heating. The chemical effects of ultrasound originate from acoustic cavitation and collapsing of generated micro-bubbles in liquid medium, which leads to a micro-mixing effect. This phenomenon increases the secondary nucleation rates and enhances mass transfer that eventually increases crystal growth rates.[29] Belviso *et al.*, found that ultrasound irradiation accelerates the dissolution of the Na silicate and aluminosilicate formed with NaOH pre-fusion. This resulted in Al–Si supersaturation, which produced higher nucleation rate of crystalline phases to be involved in zeolite synthesis.[30]

The focus of this study was to develop green synthesis approach for synthesis of valuable zeolitic materials from coal fly ash using a microwave-assisted method. The zeolites were used for the removal of ammonium from urine. The influence of various parameters such as adsorbent dosage, contact time and pH on the performance of the adsorbents were studied. Adsorption isotherms and kinetics were also studied to better understand the mechanisms and rates of adsorption.

# Methods

### Materials

Sodium hydroxide (97%), sodium aluminate (90%), calcium chloride (90%), potassium chloride (99.5%), hydrogen potassium phosphate (99.5%), and urea (99.4%) were purchased from Sigma Aldrich (Darmstadt, Germany). Hydrochloric acid (35%), magnesium chloride (99.99%), sodium chloride (99.6%), sodium sulfate (99.2), trisodium citric acid (99.2%), sodium oxalate (99.99%) and ammonium chloride (99.99%) were purchased from VWR prolab chemicals (Pennsylvania, USA). Creatine (98%) was purchased from Alfa Aesar (Massachusetts, USA). Clinoptilolite was received from Pratley Perlite Mining Company (Gauteng, South Africa), coal fly ash was supplied by Duvha Thermal Power Plant (Mpumalanga, South Africa). All chemicals were AR grade and used as received without any further purification.

# Experimental

### Zeolite preparation

The zeolites were synthesized using coal fly ash using a unique process of combining microwaves and ultrasound. Typically, 20 g of raw coal fly ash and 5 g of NaOH were transferred into a conical flask and mixed with 125 ml of distilled water. The resulting slurry was subjected to microwave irradiation for 20 min at a constant temperature (100 °C) using Sineo UWave-1000 microwave with the power set at 300 W. Thereafter, it was filtered and the obtained clear extract and solid materials were separated. Subsequently, 28 ml of the prepared $NaAlO_2$ solution was added to the clear extract (filtrate) to adjust the Si/Al ratio, in order to improve crystallization of zeolite phases.[31] To achieve crystallization, the extract solution was irradiated at 600 W for 20 min with ultrasound using the same microwave instrument. In a separate (reverse method) experiment, ultrasound irradiation followed by microwave irradiation was performed. In this method, the solution obtained was not filtered and the Si/Al ratio in the slurry was adjusted using the same $NaAlO_2$

Table 1 Technologies of ammonia removal from urine

| Technology | Approach | Removal efficiency (%) | Ref. |
|---|---|---|---|
| Air-stripping | Stripping column having a 1 m diameter and 2.5 m packing height | 97 | 12 |
| Ion-exchange/adsorption | Natural zeolite material (clinoptilolite) | 97 | 13 |
| Nitrification–denitrification | Membrane bioreactor | 90 | 14 |
| Gas separation membrane | 60 membrane surface area/reactor volume ratio, at 35 °C feed temperature with 350 L $m^{-2}$ $h^{-1}$ acid and in 8 h' hydraulic retention time | 85 | 15 |
| Forward osmosis and membrane distillation | Fresh urine (ammonia removed as urea) | 55 | 16 |
| Electrochemical oxidation | Thermally decomposed iridium oxide film anode | 40 | 17 |
| Bioelectrochemical system | Microbial fuel cell (MFC) and a microbial electrolysis cell (MEC) | 30 | 18 |

solution. Solution crystallization was performed as above. The products were centrifuged and the separated crystals (zeolites) obtained were dried in an oven at 100 °C for 24 h.

The elemental composition, crystallinity, morphology, and specific surface area of the coal fly ash and as-synthesized zeolites were characterized using X-ray fluorescence (XRF, NEX CG Rigaku), X-ray diffraction spectroscopy (XRD, Rigaku 124 Ultimate IV X-ray diffractometer), scanning electron microscopy (SEM, JEOL STM-IT300) and Brunauer–Emmett–Teller (BET, 3Flex surface area analyser) respectively. Cation exchange capacity was determined using a procedure adopted from Musyoka *et al.*[32] The concentrations of exchangeable cations ($Na^+$, $K^+$, $Mg^{2+}$ and $Ca^{2+}$) in the final solution were determined by using 930 Compact IC Flex Metrohm ion chromatography.

### Preparation of synthetic urine

Synthetic human urine (similar to that of a normal healthy adult) is characterized by 11 solutes in concentration. However, synthetic urine is free from organic macromolecules (matrix), pyrophosphates and unspecified substances that can potentially enhance or inhibit the nutrient recovery.[2] To prepare synthetic urine for use in this study, a desired mass of each salt was weighed and added into a volumetric flask and dissolve with distilled water. The salts were stirred until complete dissolution was attained. The concentrations of the solutes constituting the synthetic urine are presented in Table 2. The salt concentrations presented in Table 2 are based on measured masses and are thus theoretical. The actual concentration of the ions of interest measured using ion chromatography are presented in Table 5.

Table 2 Composition of synthetic urine prepared in this study

| Salt | Formula | Concentration (mg $L^{-1}$) |
|---|---|---|
| Calcium chloride | $CaCl_2 \cdot 2H_2O$ | 650 |
| Magnesium chloride | $MgCl_2 \cdot 6H_2O$ | 650 |
| Sodium chloride | NaCl | 4600 |
| Sodium sulfate | $Na_2SO_4$ | 2300 |
| Trisodium citric acid | $C_6H_5O_7 \cdot 2H_2O \cdot 3Na$ | 650 |
| Sodium oxalate | $Na_2$–$(COO)_2$ | 20 |
| Hydrogen potassium phosphate | $KH_2PO_4$ | 4200 |
| Potassium chloride | KCl | 1600 |
| Ammonia chloride | $NH_4Cl$ | 1000 |
| Urea | $NH_2CONH_2$ | 25 000 |
| Creatine | $C_4H_7N_3O$ | 1100 |

### Preparation of hydrolyzed urine

Fresh urine was collected from source separate male toilets at Ghent University (Belgium) and upon storage in plastic bottles, it was biologically hydrolyzed by urease bacteria. The urea was hence converted to ammonium ions according to eqn (1).

$$NH_2(CO)NH_2 + 3H_2O \xrightarrow{\text{urease}} 2NH_4^+ + HCO_3^- + OH^- \quad (1)$$

### Analytical methods

The concentrations of $Na^+$, $K^+$, $Mg^{2+}$, $Ca^{2+}$ and $NH_4^+$ present in synthetic urine and hydrolyzed urine before and after adsorption were determined using a 930 Compact IC Flex Metrohm ion chromatography. The solution pH was determined using Hanna ISE pH meter.

### Batch ammonium adsorption

The batch experiments for adsorption of the synthetic and hydrolyzed urea were conducted using clinoptilolite, coal fly ash and the as-synthesized zeolites. 25 mL of synthetic or hydrolyzed urine were transferred into conical flasks containing a desired mass of the adsorbent. The mixture was stirred on an Edmund Buhler sm-30 thermostatic shaker at room temperature for a specific period. The effect of adsorbent dose (0.2–1 g), contact time (10–120 min) and pH (2–10) were studied. To determine the rate of adsorption of ammonium on the zeolites, the kinetic studies were performed using the pseudo first order and pseudo second order models. Furthermore, Langmuir and Freundlich isotherms were conducted to understand the mechanism of ammonium adsorption onto zeolites.

The amount of ammonium ion removal capacity per unit mass of the adsorbent ($q$) and percentage ammonium removal were calculated using eqn (2) and (3) respectively.

$$q = \frac{(C_0 - C_e)V}{m} \quad (2)$$

$$\%\ \text{Removal efficiency} = \frac{C_0 - C_e}{C_0} \times 100 \quad (3)$$

Table 3 The nomenclature of the parameters and constants used in the study

| Parameter | Description | Constant | Description |
|---|---|---|---|
| $C_0$ | Initial concentration (mg $l^{-1}$) | $K_1$ | Rate constant of pseudo 1st order ($min^{-1}$) |
| $C_e$ | Ammonium ions concentration at equilibrium (mg $l^{-1}$) | $K_2$ | Rate constant of pseudo 2nd order (g $mg^{-1}$ $min^{-1}$) |
| $V$ | Sorbent volume (ml) | $q_{max}$ | Maximum uptake of ammonium ion exchange (mg $l^{-1}$) |
| $m$ | Mass of absorbent (mg) | $K_L$ | Langmuir constant (l $mg^{-1}$) |
| $q_e$ | Amount of ammonium ions adsorbed at equilibrium (mg $g^{-1}$) | $K_F$ | Freundlich constant (l $mg^{-1}$) |
| $q_t$ | Amount of ammonium ions adsorbed at a given time (mg $g^{-1}$) | $1/n$ | Heterogeneity factor |
| $t$ | Time (min) | $R^2$ | Coefficient of determination |

 

Table 4 X-ray fluorescence results of South African coal fly ash illustrating the major elements

| Compound | Mass% |
|---|---|
| $SiO_2$ | 46.9 |
| $Al_2O_3$ | 31.3 |
| FeO | 4.98 |
| CaO | 4.33 |
| $Fe_2O_3$ | 2.96 |
| $TiO_2$ | 1.54 |
| $K_2O$ | 0.72 |
| MgO | 0.60 |
| $P_2O_5$ | 0.47 |
| $SO_3$ | 0.40 |
| SrO | 0.12 |
| BaO | 0.11 |
| $V_2O_5$ | 0.06 |
| MnO | 0.03 |
| $Cr_2O_3$ | 0.03 |
| $Co_2O_3$ | 0.01 |
| $Y_2O_3$ | 0.01 |
| Loss on ignition | 4.89 |
| Total | 99.46 |
| Si/Al | 1.50 |

The pseudo first order (eqn (4)) and pseudo second order (eqn (5)) are presented.

$$\log(q_e - q_t) = \log q_e - K_1 t \quad (4)$$

$$\frac{t}{q_t} = \frac{1}{K_2 {q_e}^2} + \frac{t}{q_e} \quad (5)$$

The linear form equation of Langmuir isotherm is represented by eqn (6).

$$\frac{C_e}{q_e} = \frac{1}{q_{max} K_L} + \frac{C_e}{q_{max}} \quad (6)$$

The $q_{max}$ and $K_L$ were calculated from the slope and intercept from the graph $C_e$ *versus* $C_e/q_e$.

The linear form of Freundlich isotherm is represented by:[3]

$$\log q_e = \log K_F + \frac{1}{n} \log C_e \quad (7)$$

The summarized nomenclature of the parameters and constants used in the current study is provided in Table 3.

# Results and discussion

### Elemental composition of the zeolites

The raw coal fly ash was classified as Class F because the sum of $SiO_2$, $Al_2O_3$ and FeO was greater than 70% (Table 4). This elemental composition is typical of coal fly ash obtained from the combustion of South African bituminous coal.[33] The Si/Al ratio was found to be 1.50. This ratio is important because it governs the type of zeolite that can be synthesized from the coal fly ash.

In Fig. 1, XRD and SEM images of clinoptilolite (Fig. 1a), coal fly ash (Fig. 1b), products obtained using the microwave-ultrasound method (Fig. 1c) and products obtained using the ultrasound-microwave (reverse) methods (Fig. 1d) are presented. The SEM analysis showed irregular shaped particles of clinoptilolite (Fig. 1a), while raw fly ash showed smooth spherical particles due to the glassy crystals that covered the surface (Fig. 1b). The dominant crystal phases for clinoptilolite were clinoptilolite and albite (Fig. 1a). While fly ash had mullite and quartz as its dominant crystal phases as shown by the XRD profile (Fig. 1b). The morphology and crystal structure of coal fly ash was transformed significantly by microwave and ultrasound irradiations. Pure phase sodalite phases were formed when the microwave-ultrasound irradiation method was used (Fig. 1c). Some spherical flower-like structures that are associated with sodalite were observed.

The 'reverse method' gave mixed phase sodalite with impurities of coal fly ash phases (Fig. 1d). Sodalite crystals forming on top of the coal fly ash particles were observed. This is because the slurry was not filtered and hence coal fly ash crystals were still present in the final sodalite product.

### Surface area and cation exchange capacity analysis of coal fly ash and its products

The surface area and the cation exchange capacity of the raw coal fly ash were 1.2 $m^2\ g^{-1}$ and 0.29 meq. $g^{-1}$ respectively (Table 5). These low values indicated that the raw coal fly ash would have a low ammonium uptake. A significant improvement in the surface area and cation exchange capacity was recorded upon zeolitization. The mixed phase sodalite had a surface area of 7.8 $m^2\ g^{-1}$ and cation exchange capacity of 1.18 meq. $g^{-1}$. Furthermore, the pure phase sodalite showed a higher surface area (16 $m^2\ g^{-1}$) and cation exchange capacity (2.92 meq. $g^{-1}$). The surface area of pure phase sodalite was comparable to that of clinoptilolite Table 5. For this reason, the pure phase sodalite and clinoptilolite were expected to show higher ammonium ion uptake. In this study, the ammonium ion removal efficiency of the synthesized zeolites was compared with that of a natural zeolite (clinoptilolite), which is known for high cation exchange capacity and selectivity towards ammonium in aqueous solutions. The clinoptilolite used in this study was characterized by surface area and cation exchange capacity of 18 $m^2\ g^{-1}$ and 2.13 meq. $g^{-1}$ respectively.

### Zeta potential of coal fly ash and its products

The zeta potential of the raw coal fly ash, clinoptilolite, and the synthesized zeolites was carried out with the sole purpose of elucidating the effect of pH on the adsorption of ammonium ions from urine and the results are presented on Fig. 2. It is worth noting that, at the surface of aluminosilicates, the anionic groups present are silicates ($O–SiO_2^-$) and aluminates ($O–AlO^-$). These functional groups are negatively charged. However, they are pH dependent and can undergo protonation or deprotonation as a function of pH.[34] The isoelectric point (IEP) (*i.e.* pH of neutral charge) of coal fly ash, clinoptilolite,

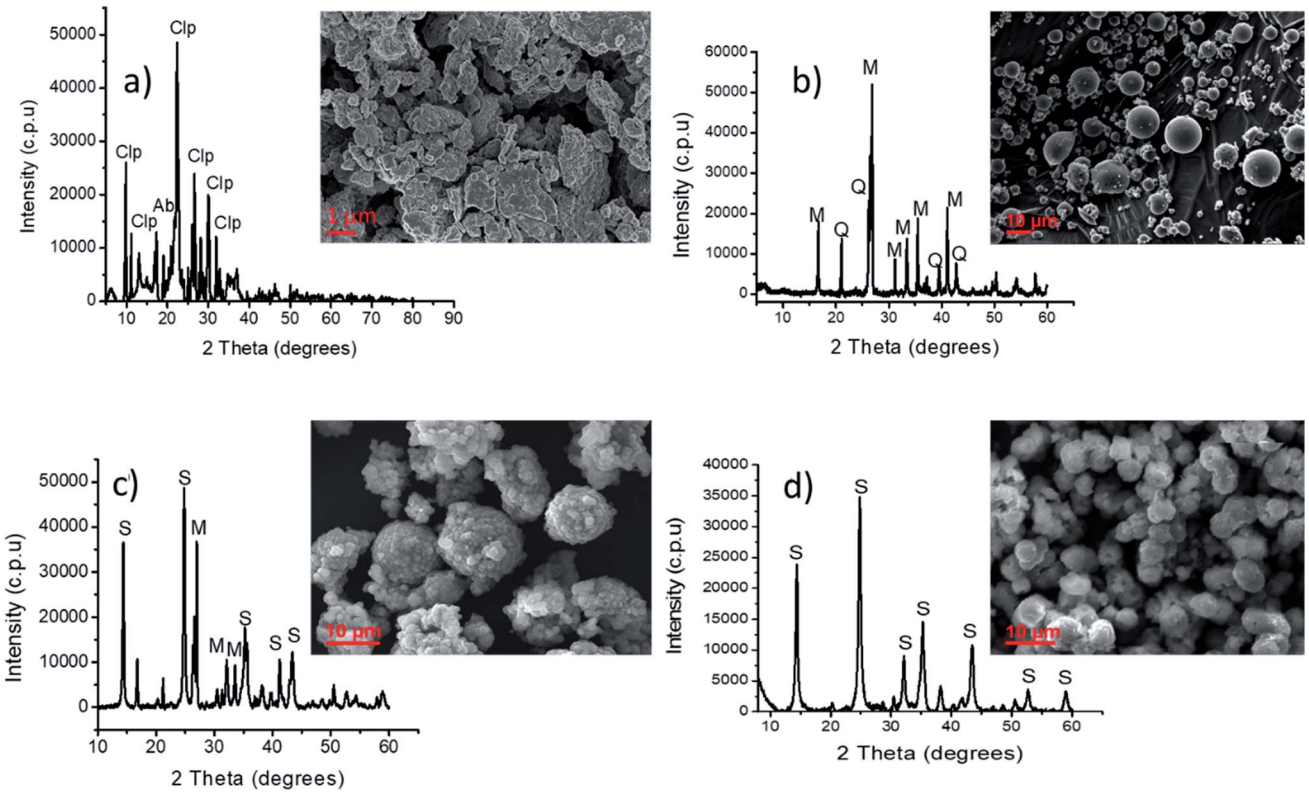


Fig. 1 XRD plots and SEM images of (a) clinoptilolite, (b) raw coal fly ash, and its synthesized products (c) sodalite and (d) pure phase sodalite (Clp = clinoptilolite, Ab = albite, M = mullite, Q = quartz, S = sodalite).

mixed phase sodalite (MS) and pure phase sodalite (S) was determined as 4.7, 7.9, 6.3 and 6.8 respectively. The negative charge of all the materials increased rapidly with an increase in pH beyond the IEP. The negative charge of the zeolites has a direct impact on the adsorption of the positively charged ions. Specifically, the positively charged ions are attracted to the negatively charged surface of the zeolites, *i.e.* a process known as an electrostatic interaction.

Table 5 Surface area, pore volume and cation exchange capacity of clinoptilolite, raw coal fly ash and synthesized zeolitic products

| Material | BET surface area ($m^2\ g^{-1}$) | Pore volume ($m^3\ g^{-1}$) | CEC (meq. $g^{-1}$) |
|---|---|---|---|
| Coal fly ash | 1.1965 | 0.001109 | 0.29 |
| Clinoptilolite | 17.8972 | 0.029877 | 2.13 |
| Mixed sodalite | 7.8100 | 0.018864 | 1.18 |
| Sodalite | 15.5000 | 0.034826 | 2.92 |

## Removal of ammonia from synthetic urine and hydrolyzed urine

The concentration of ammonium and selected ions before and after adsorption is presented in Table 6. A higher removal of $NH_4^+$ compared with the other cations ($K^+$, $Na^+$ and $Ca^{2+}$) in both synthetic and hydrolyzed urine was observed. This was due to the high concentration of $NH_4^+$ which subsequently ensured greater driving force for adsorption.[35] The $Mg^{2+}$ ions were not

Table 6 Characterization of synthetic and hydrolyzed urine before and after adsorption[a]

| Parameters | Synthetic urine before adsorption | Synthetic urine after adsorption | | | | Hydrolyzed urine before adsorption | Hydrolyzed urine after adsorption | | | |
|---|---|---|---|---|---|---|---|---|---|---|
| | | CFA | MS | Clin | Sod | | CFA | MS | Clin | Sod |
| $NH_4^+$–N (mg $l^{-1}$) | 215.2 | 131.1 | 87.41 | 51.24 | 39.01 | 723.5 | 476.1 | 415.3 | 225.6 | 215.7 |
| $Ca^{2+}$ (mg $l^{-1}$) | 28.12 | 30.62 | 33.20 | 54.33 | 48.07 | 93.01 | 88.02 | 96.77 | 103.0 | 118.2 |
| $K^+$ (mg $l^{-1}$) | 153.3 | 150.3 | 149.0 | 115.3 | 120.4 | 213.4 | 210.5 | 186.3 | 160.3 | 181.4 |
| $Mg^{2+}$ | ND | 8.323 | 20.10 | 66.63 | 4.114 | ND | 11.07 | 22.06 | 65.55 | 57.06 |
| $Na^+$ (mg $l^{-1}$) | 92 | 86.22 | 112.8 | 103.7 | 126.0 | 127.6 | 120.9 | 136.4 | 160.8 | 203.2 |

[a] ND: not detected; CFA: coal fly ash, MS: mixed sodalite, Clin: clinoptilolite, Sod: sodalite.

 

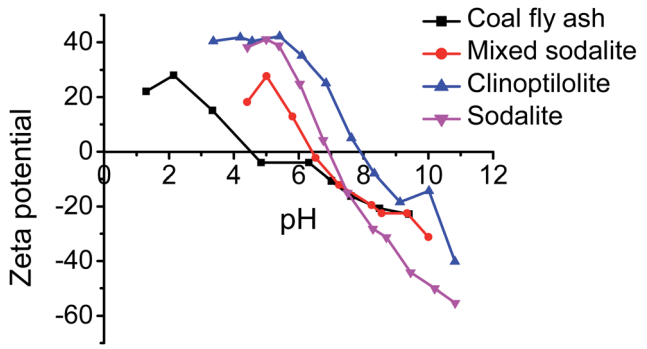


Fig. 2 pH *vs.* zeta potential of raw coal fly ash, clinoptilolite, mixed-phase sodalite and pure phase sodalite.

detected from both synthetic urine and hydrolyzed urine due to the dilution effect. However, $Mg^{2+}$ ions were detected after adsorption. Furthermore, when adsorption was carried out using mixed sodalite, pure sodalite and clinoptilolite, the concentration of $Na^+$ and $Ca^{2+}$ ions was increased. Notably, zeolites consist of weakly bound cations which are likely to be exchanged with cations in solution.[36] This suggests that $Na^+$, $Ca^{2+}$ and $Mg^{2+}$ ions present in the zeolites were exchanged with $NH_4^+$ ions in solution. The synthetic zeolites were alkali-treated with NaOH leading to an increase in concentration of $Na^+$ ions. These ions enable ionic exchange with $NH_4^+$ from urine. Lu *et al.*, also noted that $Al^{3+}$ has stronger affinity with zeolite compared to $Na^+$, synthetic zeolite ($Na^+$ modified zeolite) demonstrated higher ion exchange capacity compared to natural zeolite for ammonium adsorption.[37] It is worth noting that ionic exchange capacity between divalent ions ($Mg^{2+}$ and $Ca^{2+}$) and $NH_4^+$ ions from an exchange surface is lower than the exchange between two monovalent cations such as $Na^+$ ions.[35] This explains the high ammonium ion removal efficiency by sodalite due to the high amount of monovalent $Na^+$ ions induced by NaOH treatment. Nonetheless, the concentration of $K^+$ ions in solution was reduced after adsorption indicating possible re-adsorption by the adsorbents due to its strong affinity to zeolites.[38] On the other hand, coal fly ash demonstrated minimal cation exchange due to its low cation exchange capacity and therefore displayed the lowest ammonium ion removal (Table 6). Ion-exchange was not the only controlling mechanism during the adsorption process. This is because the major ions ($Na^+$, $K^+$, $Ca^{2+}$ and $Mg^{2+}$) released from the adsorbents to the solution were not equivalent to the $NH_4^+$ ions adsorbed. It is therefore believed that molecular adsorption was involved in the removal of $NH_4^+$ ion from the urine samples.

### Effect of adsorbent dosage

To study the effect of adsorbent dosage, experiments were carried out at a neutral pH of 7 for 30 min at room temperature (25 °C), while dosage was varied from 0.2–1 g. Fig. 3 shows the effect of adsorbent dosage on the removal ammonium from synthetic and hydrolyzed urine. Raw coal fly ash, clinoptilolite and coal fly ash-derived zeolitic products were evaluated as adsorbents. A proportional increase in ammonium removal with an increase in adsorbent dosage was observed in all cases. This increase in ammonium uptake was attributed to the increased number of exchangeable and active adsorption sites.[9] Xu *et al.*, also observed an increase in ammonia removal efficiency from 2% to 55% with an increase in zeolite adsorbent dosage of 4 g $l^{-1}$ to 10 g $l^{-1}$ respectively.[39] It is worth noting that understanding the effect of adsorbent dosage facilitate the determination of the most effective amount of adsorbent for a given volume of urine. Due to its porous nature, high cation exchange capacity and surface area (Table 5), sodalite presented the highest ammonium removal efficiency from synthetic urine (82%) and hydrolyzed urine (73%). The porosity and cation exchange capacity of sodalite were improved during microwave treatment which subsequently led to the high uptake of the ammonium ions from solution. Likewise, clinoptilolite showed high ammonium removal efficiencies of up to 78% from synthetic urine and 70% from hydrolyzed urine due to its high cation exchange capacity and ammonium ion selectivity. On the other hand, the mixed phase sodalite adsorbent showed low removal efficiencies due to its low crystallinity and the presence of coal fly ash phases (Fig. 1c). This was as a result of its low

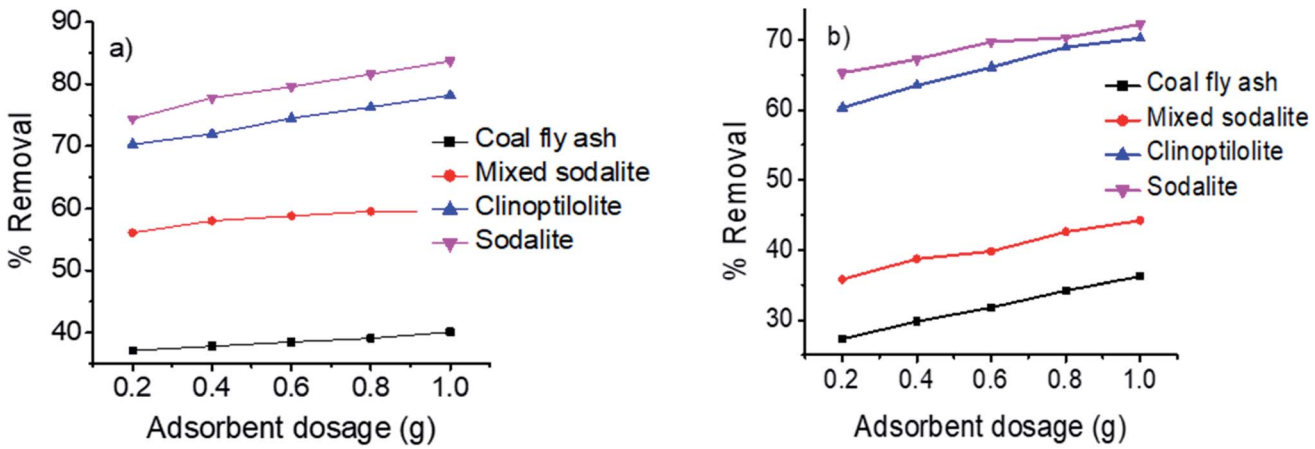


Fig. 3 Effect of adsorbent dosage on the removal of ammonium from (a) synthetic urine and (b) hydrolyzed urine.

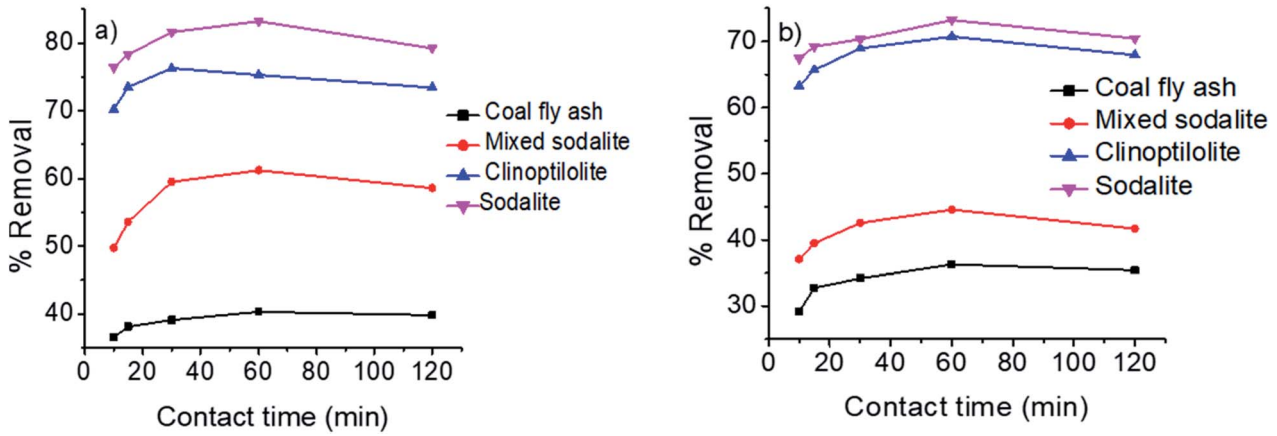


Fig. 4 Effect of contact time on the removal of ammonium from (a) synthetic urine and (b) hydrolyzed urine.

cation exchange capacity and surface area a raw coal fly-ash demonstrated the lowest removal efficiency (Table 5). Comparably, the removal efficiency was reduced when hydrolyzed urine was used instead of synthetic urine. This phenomenon was attributed to the presence of organic macromolecules (matrix) and pyrophosphates in hydrolyzed urine.[2] These macromolecules are believed to hinder the diffusion of ammonium ions to active adsorption sites of the adsorbent. The findings of this study were relatively comparable to the results reported by (Zhang *et al.*).[23]

### Effect of contact time

The effect of contact time was performed at constant pH of 7, absorbent dosage of 1 g at room temperature of 25 °C, while contact time was varied from 10–120 min. Fig. 4 presents the effect of contact time on the removal of ammonium from synthetic and hydrolyzed urine using coal fly ash, clinoptilolite and the synthesized zeolitic products. The percentage removal of ammonium ion increased with an increase in contact time. Notably, a rapid ammonium removal occurred from 10 min to 30 min. This was attributed to high solute gradient and abundant vacant adsorbent sites at the beginning of experiment leading to high driving force for ammonium ions to diffuse to the exchangeable sites. Previous studies has shown that ammonium uptake by zeolites is a fast process and it can attain equilibrium in short times (*e.g.* 10–15 min).[25] This is similar to results reported by Xue *et al.*, where 66% of ammonia was removed after 5 min of contact time. However, only 5% increase in removal efficiency was observed after 1440 min.[40] Beyond 30 min, the rate of ammonium removal proceeded at a slower rate until equilibrium was attained at 60 min. This observation was explained by the saturation of active adsorption sites.[9] All other adsorbents attained equilibrium at 60 min except sodalite which attained equilibrium at 30 min for synthetic urine. However, sodalite desorbed ammonium back to solution beyond 60 min of agitation. This observation was due to that sodalite is a cation exchange material. The framework cations (*i.e.* $Na^+$, $Ca^{2+}$) that exchanged with $NH_4^+$ ions can readily exchange back to attain a neutral state. Nonetheless, the $NH_4^+$ percentage removal by coal fly ash did not reduce after equilibrium due to its low cation exchange capacity.

### Effect of pH

The effect of pH studied at optimum conditions of 1 g adsorbent dosage, 60 min contact time at room temperature (25 °C), while varying the pH between 2–10. According to the zeta potential

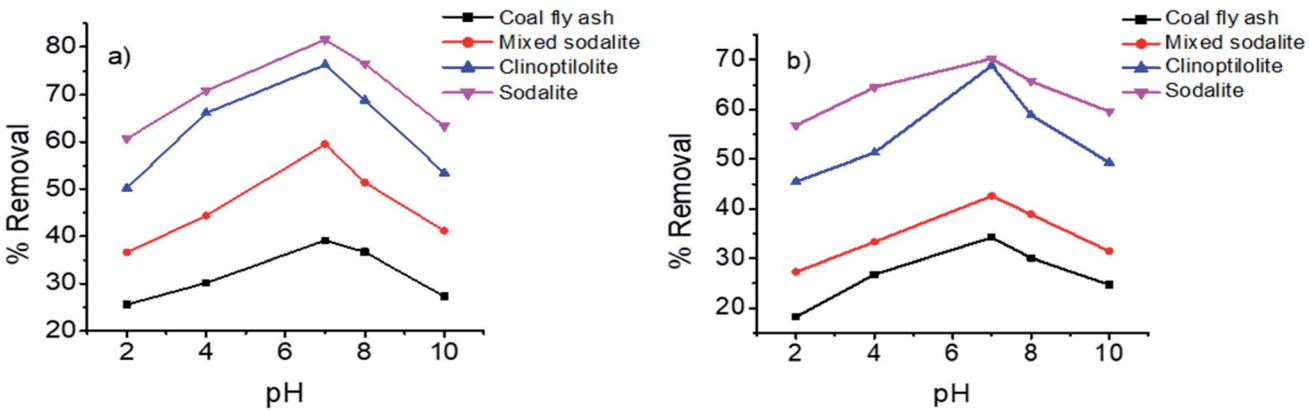


Fig. 5 Effect of pH on the removal of ammonium from (a) synthetic urine and (b) hydrolyzed urine.

 

results, the adsorbents became more negatively charged at higher pH values. The negative surface charge was desired for the removal of ammonium from urine. Following the zeta potential results, the adsorption of ammonium ions on various adsorbents was carried out at the pH range of 2–10 and the results are presented on Fig. 5. The removal efficiency increased from the acidic pH (*i.e.* pH 2) to neutral pH of 7. A further increase in pH (8–10) led to a decrease in ammonium adsorption. Remarkably, the zeta potential results showed that the zeolites became negatively at the higher pH values (*i.e.* pH > IEP) (Fig. 2). In acid medium, the low removal efficiency was attributed to the positive surface charge resulting in the repulsive forces between the adsorbent surface and positively charged $NH_4^+$ ions. This decrease in ammonia removal at low pH was also reported by Liu *et al.*, and it was attributed to the dissolution or collapse of the zeolite structure at pH levels below 4.[41] Likewise, Hermassi *et al.*, reported a similar trend where the optimum pH for ammonium removal was between pH 4 and 8.5.[42] An increase in pH beyond the characteristic optimal values affects the adsorption properties of the zeolites and exchanging ions, leading to a decrease in adsorption capacity.[43] The $NH_4^+$ ions were converted to $NH_3$ at higher pH values leading to a decrease ion exchange capacity with the zeolitic materials.[44] Likewise, different forms of ammonia in solution affects the surface charge of the adsorbent as well as the degree of ionization and speciation of the adsorbate.[45] Therefore, a neutral pH (*i.e.* pH 7) was optimal for removal of ammonium ions from urine. These findings were in agreement with the previously reported study.[46] Sun *et al.*, also observed high selectivity of ammonium ions on an aluminosilicate adsorbent at pH 7 and an optimum removal efficiency of 99% was recorded.[47]

### Adsorption kinetics

Adsorption kinetics are crucial as they provide information about the reaction pathways.[48] The exchange of ammonium ions on coal fly ash, clinoptilolite and the synthesized zeolitic products was modeled using pseudo first order and pseudo second order kinetics. The rate constants were calculated from the slope and intercept of the graph (Fig. 6). The $R^2$ values of the linearized plots were used to determine the kinetic model that best fits the adsorption of ammonium onto the zeolites.

Based on the $R^2$ values, the adsorption of ammonium on all adsorbents followed pseudo-second-order kinetics with coefficient of determination ($R^2$ > 0.99) higher than those of the pseudo-first-order kinetics ($R^2$ < 0.96) (Table 7). The same results were observed by Xin *et al.*, where the removal of ammonia from aqueous solution using a zeolite adsorbent was reported to follow a pseudo-second-order kinetics with 0.9973 coefficient of determination.[49] The pseudo second order

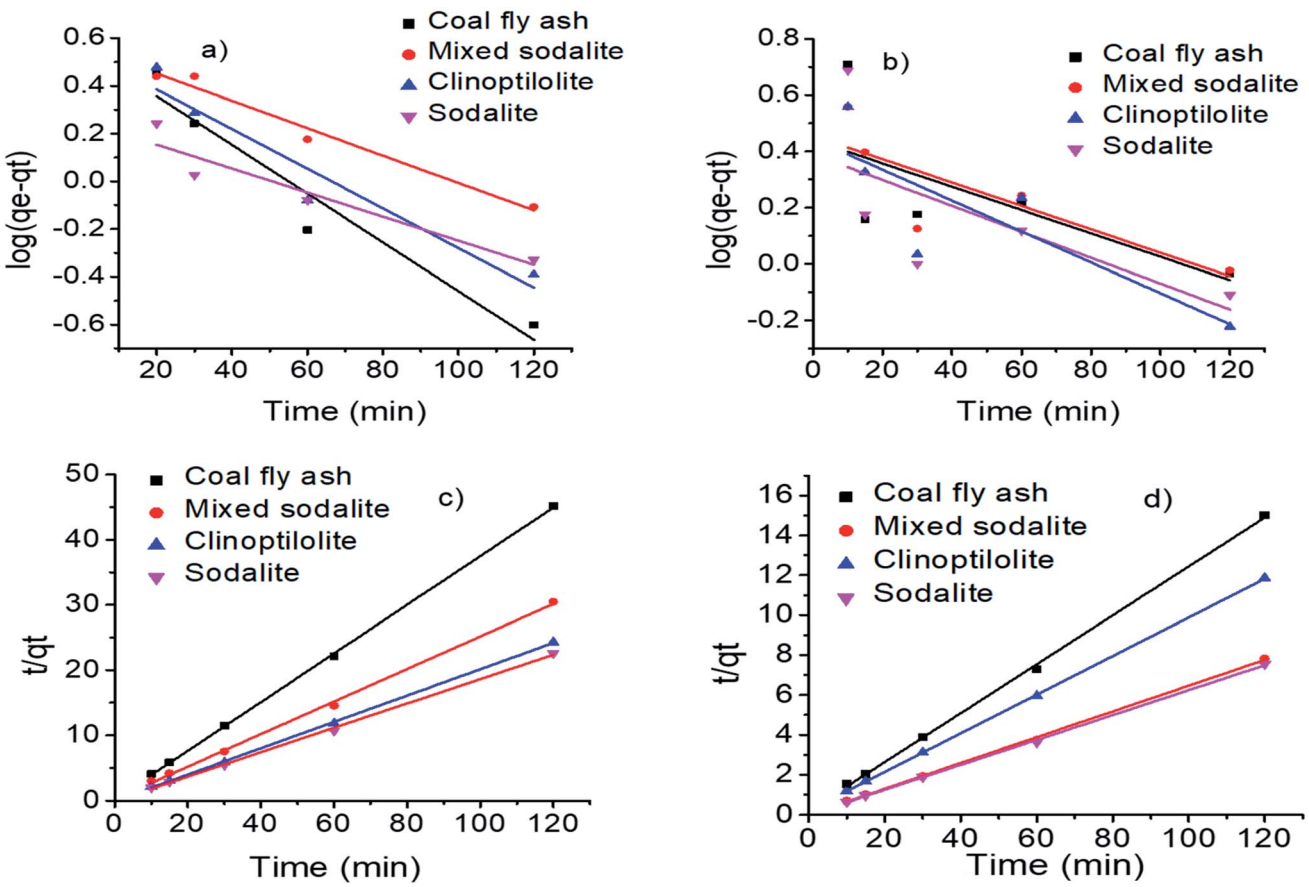


Fig. 6 First order kinetics for (a) synthetic urine and (b) hydrolyzed urine and second order kinetics (c) synthetic urine (d) hydrolyzed urine.

Table 7 Rate constants and correlation coefficients for the studied kinetics models

| Pseudo first order | | | | | | | |
|---|---|---|---|---|---|---|---|
| Synthetic urine | | | | Hydrolyzed urine | | | |
| Material | $K_1$ (min$^{-1}$) | $q_e$ (mg g$^{-1}$) | $R^2$ | Material | $K_1$ (min$^{-1}$) | $q_e$ (mg g$^{-1}$) | $R^2$ |
| Coal fly ash | 3.638 | 0.020 | 0.91568 | Coal fly ash | 2.458 | 0.391 | 0.27644 |
| Mixed sodalite | 3.684 | 0.011 | 0.96674 | Mixed sodalite | 2.458 | 0.391 | 0.27644 |
| Clinoptilolite | 3.556 | 0.016 | 0.90264 | Clinoptilolite | 2.786 | 0.005 | 0.60286 |
| Sodalite | 1.799 | 0.010 | 0.8629 | Sodalite | 2.458 | 0.391 | 0.27644 |
| **Pseudo second order** | | | | | | | |
| Synthetic urine | | | | Hydrolyzed urine | | | |
| Material | $K_2$ (mg g$^{-1}$ min$^{-1}$) | $q_e$ (mg g$^{-1}$) | $R^2$ | Material | $K_2$ (mg g$^{-1}$ min$^{-1}$) | $q_e$ (mg g$^{-1}$) | $R^2$ |
| Coal fly ash | 0.809 | 2.679 | 0.99962 | Coal fly ash | 0.081 | 8.159 | 0.99962 |
| Mixed sodalite | 0.306 | 4.006 | 0.9983 | Mixed sodalite | 0.907 | 15.48 | 0.9991 |
| Clinoptilolite | 0.628 | 4.948 | 0.99956 | Clinoptilolite | 0.0448 | 10.33 | 0.99989 |
| Sodalite | 0.403 | 5.534 | 0.99874 | Sodalite | 0.897 | 16.03 | 0.99924 |

suggests that the adsorption rate was governed by chemical adsorption mechanism.[50] Therefore, the ammonium adsorption process was affected by the chemical properties of the zeolite and urine leading to an ion exchange being the rate-determining step and subsequently resulting in longer periods for ammonium uptake.[23] The adsorption capacity ($q_e$) was highest for sodalite which agreed with the high ammonium removal efficiency obtained compared to the other adsorbents.

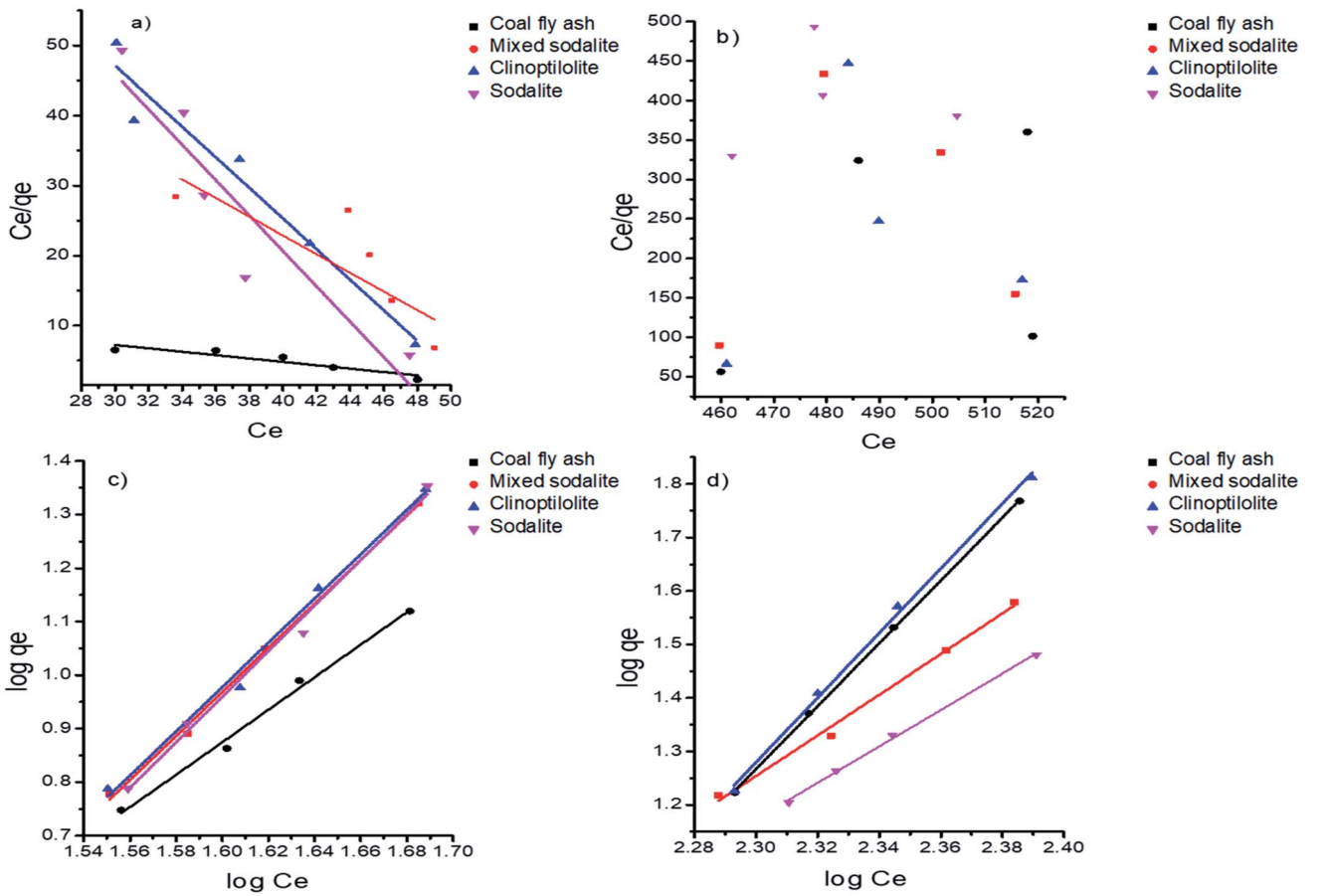


Fig. 7 Langmuir isotherm for (a) synthetic urine and (b) hydrolyzed urine; and Freundlich isotherm for (c) synthetic urine and (d) hydrolyzed urine.

 

Table 8 The constants and correlation coefficients for the isotherm models

| Langmuir | | | | | | | |
|---|---|---|---|---|---|---|---|
| Synthetic urine | | | | Hydrolyzed urine | | | |
| Material | $q_{max}$ (mg g$^{-1}$) | $K$ (L mg$^{-1}$) | $R^2$ | Material | $q_{max}$ (mg g$^{-1}$) | $K$ (L mg$^{-1}$) | $R^2$ |
| Coal fly ash | 4.132 | $6.05 \times 10^{-4}$ | 0.81452 | Coal fly ash | N/A | N/A | N/A |
| Mixed sodalite | 0.362 | 0.191 | 0.5365 | Mixed sodalite | N/A | N/A | N/A |
| Clinoptilolite | 3.116 | 0.015 | 0.9409 | Clinoptilolite | N/A | N/A | N/A |
| Sodalite | 0.912 | 0.011 | 0.8207 | Sodalite | N/A | N/A | N/A |
| Freundlich | | | | | | | |
| Synthetic urine | | | | Hydrolyzed urine | | | |
| Material | $K_F$ (mg g$^{-1}$) (mg L$^{-1}$)$^{1/n}$ | $1/n$ | $R^2$ | Material | $K_F$ (mg g$^{-1}$) (mg L$^{-1}$)$^{1/n}$ | $1/n$ | $R^2$ |
| Coal fly ash | 0.36 | 0.33 | 0.9962 | Coal fly ash | 0.016 | 0.13 | 0.9995 |
| Mixed sodalite | 0.44 | 0.62 | 0.9886 | Mixed sodalite | 0.087 | 0.25 | 0.997 |
| Clinoptilolite | 1.12 | 0.35 | 0.9876 | Clinoptilolite | 0.56 | 0.18 | 0996 |
| Sodalite | 1.89 | 0.29 | 0.9433 | Sodalite | 0.93 | 0.22 | 0.991 |

The increase in $q_e$ with an increase in initial ammonium concentration, was higher for hydrolyzed urine compared to synthetic urine. This was due to the existence of equilibrium between the liquid phase concentration (urine) and the adsorption capacity of the zeolite. An increase in the initial ammonium ion concentration resulted in the equilibrium shifting towards a higher adsorption capacity region.[51] The $q_e$ values for the pseudo second order were closer to the experimental values, showing that pseudo second order was the best fitting adsorption kinetics.

### Adsorption isotherms

Adsorption isotherms are important because they provide adsorption mechanism for the interaction between the adsorbent and the adsorbate.[52] The Langmuir and Freundlich isotherms were used models to study the adsorption mechanism of ammonium on coal fly ash, clinoptilolite and the synthesized zeolite products. The Langmuir isotherm assumes that adsorption occurs at specific homogeneous sites within the adsorbent, meaning the adsorbate forms monolayer onto the surface of the adsorbent.[53] Moreover, Freundlich isotherms describes the formation of the multiple layers on the surface of the adsorbent.[48] The constants were calculated from the slope and intercept of the graph (Fig. 7). The Langmuir constants for adsorption of ammonium on zeolites were in the range of 0.00061 to 0.19 L g$^{-1}$ while those of the Freundlich isotherm ranged between 0.13 and 1.89 mg g$^{-1}$. The coefficient of determination ($R^2$) demonstrated a better fit on the linear plots of Freundlich isotherm model as opposed to those of Langmuir (Table 8); suggesting that the adsorption of ammonium onto zeolites followed the Freundlich isotherm. He *et al.*, found ammonia adsorption on synthesized zeolites to favor Freundlich isotherm, which is in agreement with the results obtained in this study. The findings suggested a non-uniform distribution of adsorption energy over the surface of the zeolite adsorbent.[54] Similarly, the heterogeneity factor $1/n$ was between 0–1 suggesting that the adsorption process was favorable.

## Conclusions

Greener energy efficient processes involving microwave and ultrasound irradiation were developed to synthesize sodalite zeolite materials from coal fly ash biomass waste. It was observed that raw coal fly is not an effective adsorbent for ammonium in solution and urine. Pure phase sodalite with relatively high surface area (16 m$^2$ g$^{-1}$) and CEC (2.92 meq. g$^{-1}$) exhibited higher ammonium removal efficiency (up 82%) compared to natural zeolite (clinoptilolite). The adsorption process followed the Freundlich isotherm and the pseudo 2$^{nd}$ order kinetic model. The coal fly ash derived zeolites offer a great opportunity in environmental remediation as low-cost adsorbent.

## Conflicts of interest

There are no conflicts to declare.

## Acknowledgements

The authors would like to acknowledge the University of South Africa, SabiNano (Pty) Ltd and DST/MINTEK Nanotechnology Innovation Centre for supporting this work.

## References

1 C. Rose, A. Parker, B. Jefferson and E. Cartmell, The Characterization of Feces and Urine: A Review of the

Literature to Inform Advanced Treatment Technology, *Crit. Rev. Environ. Sci. Technol.*, 2015, **45**, 1827–1879.
2 B. Lind, Z. Ban and S. Bydén, Nutrient recovery from human urine by struvite crystallization with ammonia adsorption on zeolite and wollastonite, *Bioresour. Technol.*, 2000, **73**, 169–174.
3 J. Soetardji, *et al.*, Ammonia removal from water using sodium hydroxide modified zeolite mordenite, *RSC Adv.*, 2015, **5**, 83689–83699.
4 X. Zhou, *et al.*, Simultaneous Current Generation and Ammonium Recovery from Real Urine Using Nitrogen-purged Bioelectrochemical Systems, *RSC Adv.*, 2015, **5**, 86.
5 K. Xu, C. Wang, H. Liu and Y. Qian, Simultaneous removal of phosphorus and potassium from synthetic urine through the precipitation of magnesium potassium phosphate hexahydrate, *Chemosphere*, 2011, **84**, 207–212.
6 B. Liu, A. Giannis, J. Zhang, V. Chang and J. Wang, Air stripping process for ammonia recovery from source-separated urine: Modeling and optimization, *J. Chem. Technol. Biotechnol.*, 2015, **90**, 2208–2217.
7 K. Udert and M. Wächter, Complete nutrient recovery from source-separated urine by nitrification and distillation, *Water Res.*, 2012, **46**, 453–464.
8 Q. Chen, *et al.*, Removal of ammonia from aqueous solutions by ligand exchange onto a Cu(II)-loaded chelating resin: kinetics, equilibrium and thermodynamics, *RSC Adv.*, 2017, **7**, 12812–12823.
9 N. Widiastuti, H. Wu, H. Ang and D. Zhang, Removal of ammonium from greywater using natural zeolite, *Desalination*, 2011, **277**, 15–23.
10 X. Ren, *et al.*, Synthesis and characterization of a single phase zeolite A using coal fly ash, *RSC Adv.*, 2018, **8**, 42200–42209.
11 K. Margeta, N. Zabukovec, M. Šiljeg and A. Farkas, Natural Zeolites in Water Treatment – How Effective is Their Use, *Water Treat.*, 2013, **18**, 89.
12 S. Basakcilardan-Kabakci, N. Ipekoglu and I. Talinli, Recovery of Ammonia from Human Urine by Stripping and Absorption, *Environ. Eng. Sci.*, 2007, **24**, 615–624.
13 B. Beler-Baykal, A. Allar and S. Bayram, Nitrogen recovery from source-separated human urine using clinoptilolite and preliminary results of its use as fertilizer, *Water Sci. Technol.*, 2011, **63**(4), 811–817.
14 S. Yao, *et al.*, On-site nutrient recovery and removal from source-separated urine by phosphorus precipitation and short-cut nitrification-denitrification, *Chemosphere*, 2017, **175**, 210–218.
15 J. Nagy, J. Kaljunen and A. Toth, Nitrogen recovery from wastewater and human urine with hydrophobic gas separation membrane: experiments and modelling, *Chem. Pap.*, 2019, **73**, 1903–1915.
16 H. Ray, F. Perreault and T. Boyer, Urea recovery from fresh human urine by forward osmosis and membrane distillation (FO–MD), *Environ. Sci.: Water Res. Technol.*, 2019, **5**, 1993.
17 H. Zöllig, A. Remmele, E. Morgenroth and K. Udert, Removal rates and energy demand of the electrochemical oxidation of ammonia and organic substances in real stored urine, *Environ. Sci.: Water Res. Technol.*, 2017, **3**, 480.
18 M. Arredondo, *et al.*, Bioelectrochemical systems for nitrogen removal and recovery from wastewater, *Environ. Sci.: Water Res. Technol.*, 2015, **1**, 22.
19 C. Belviso, *et al.*, Synthesis of zeolites at low temperatures in fly ash-kaolinite mixtures, *Microporous Mesoporous Mater.*, 2015, **212**, 35–47.
20 C. Belviso, State-of-the art applications of fly ash from coa land biomass: A focus on zeolite synthesis processes and issues, *Prog. Energy Combust. Sci.*, 2018, **65**, 109–135.
21 C. Belviso, F. Cavalcante, F. Huertas, A. Lettino, P. Ragone and S. Fiore, The crystallisation of zeolite (X- and A-type) from fly ash at 25 °C in artificial sea water, *Microporous Mesoporous Mater.*, 2012, **162**, 115–121.
22 C. Belviso, F. Cavalcante and S. Fiore, Ultrasonic waves induce rapid zeolite synthesis in a seawater solution, *Ultrason. Sonochem.*, 2013, **20**, 32–36.
23 M. Zhang, *et al.*, Ammonium removal from aqueous solution by zeolites synthesized from low-calcium and high-calcium fly ashes, *Desalination*, 2011, **277**, 46–53.
24 C. Belviso, F. Cavalcante, A. Lettino and S. Fiore, Effects of ultrasonic treatment on zeolite synthesized from coal fly ash, *Ultrason. Sonochem.*, 2011, **18**, 661–668.
25 M. Zhang, *et al.*, Removal of ammonium from aqueous solutions using zeolite synthesized from fly ash by a fusion method, *Desalination*, 2011, **271**, 111–121.
26 M. El-Naggar, A. El-Kamash, M. El-Dessouky and A. Ghonaim, Two-step method for preparation of NaA-X zeolite blend from fly ash for removal of cesium ions, *J. Hazard. Mater.*, 2008, **154**, 963–972.
27 L. Deng, Q. Xu and H. Wu, Synthesis of Zeolite-like Material by Hydrothermal and Fusion Methods Using Municipal Solid Waste Fly Ash, *Procedia Environ. Sci.*, 2016, **31**, 662–667.
28 N. Murayama, H. Yamamoto and J. Shibata, Zeolite synthesis from coal fly ash by hydrothermal reaction using various alkali sources, *J. Chem. Technol. Biotechnol.*, 2002, **286**, 6–8.
29 T. Aldahri, J. Behin, H. Kazemian and S. Rohani, Synthesis of zeolite Na-P from coal fly ash by thermo-sonochemical treatment, *Fuel*, 2016, **182**, 494–501.
30 C. Belviso, Ultrasonic vs hydrothermal method: Different approaches to convert fly ash into zeolite. How they affect the stability of synthetic products over time?, *Ultrason. Sonochem.*, 2018, **43**, 9–14.
31 N. Musyoka, Zeolite A, X and Cancrinite from South African coal fly ash: mechanism of crystallization, routes to rapid synthesis and new morphology, MSc dissertation, University of the Western Cape, 2012.
32 N. Musyoka, *et al.*, Removal of Toxic Elements from Brine Using Zeolite Na-P1 Made from a South African Coal Fly Ash, *Int. Mine Water*, 2009, **6**, 680–687.
33 N. Musyoka and L. Petrik, Novel zeolite Na-X synthesized from fly ash a as a heterogeneous catalyst in biodiesel production, *Catal. Today*, 2012, **9**, 54–60.
34 C. Gunasekara, *et al.*, Zeta potential, gel formation and compressive strength of low calcium fly ash geopolymers, *Constr. Build. Mater.*, 2015, **95**, 592–599.

 

35 D. Wijesinghe, *et al.*, Ammonium removal from high-strength aqueous solutions by Australian zeolite, *J. Environ. Sci. Health, Part A: Toxic/Hazard. Subst. Environ. Eng.*, 2016, **4529**, 1–12.

36 N. Koshy and D. Singh, Fly ash zeolites for water treatment applications, *J. Environ. Chem. Eng.*, 2016, **4**, 1460–1472.

37 Q. Lu, *et al.*, A novel approach of using zeolite for ammonium toxicity mitigation and value-added Spirulina cultivation in wastewater, *Bioresour. Technol.*, 2019, **280**, 127–135.

38 J. Guo, Adsorption characteristics and mechanisms of high-levels of ammonium from swine wastewater using natural and MgO modified zeolites, *Desal. Water Treat.*, 2016, **57**, 5452–5463.

39 Q. Xu, *et al.*, Simultaneous removal of ammonia and phosphate using green synthesized iron oxide nanoparticles dispersed onto zeolite, *Sci. Total Environ.*, 2020, **703**, 135002.

40 R. Xue, *et al.*, Simultaneous removal of ammonia and N-nitrosamine precursors from high ammonia water by zeolite and powdered activated carbon, *J. Environ. Sci.*, 2017, **64**, 82–91.

41 Y. Liu, *et al.*, Synthesis of zeolite P1 from fly ash under solvent-free conditions for ammonium removal from water, *J. Cleaner Prod.*, 2018, **202**, 11–22.

42 M. Hermassi, *et al.*, Simultaneous ammonium and phosphate recovery and stabilization from urban sewage sludge anaerobic digestates using reactive sorbents, *Sci. Total Environ.*, 2018, **630**, 781–789.

43 A. Khosravi, M. Esmhosseini, J. Jalili and S. Khezri, Optimization of ammonium removal from waste water by natural zeolite using central composite design approach, *J. Inclusion Phenom. Macrocyclic Chem.*, 2012, **74**, 383–390.

44 X. Cui, S. Chen, X. Zhang, J. Ma and R. Li, Ammonia Removal from Aqueous Solution by Zeolites Synthesized from Coal Fly Ash, *2011 Fourth Int. Conf. Intell. Comput. Technol. Autom.*, 2011, vol. 2, pp. 806–808.

45 S. Jiang, X. Wang, S. Yang and H. Shi, Characteristics of simultaneous ammonium and phosphate adsorption from hydrolysis urine onto natural loess, *Environ. Sci. Pollut. Res.*, 2016, **23**, 2628–2639.

46 Q. Deng, Ammonia removal and recovery from wastewater using natural zeolite: an integrated system for regeneration by air stripping followed ion exchange, MSc dissertation, University of Waterloo, 2014.

47 N. Sun, W. Shi, L. Ma and S. Yu, Investigations on the mechanism, kinetics and isotherms of ammonium and humic acid co-adsorption at low temperature by 4A-molecular sieves modified from attapulgite, *RSC Adv.*, 2017, **7**, 17095.

48 L. Nthunya, M. Masheane, S. Malinga, E. Nxumalo and S. Mhlanga, Electrospun chitosan-based nanofibres for removal of phenols from drinking water, *Water SA*, 2018, **44**, 377–386.

49 G. Xin, M. Wang, L. Chen, Y. Zhang and M. Wang, Synthesis and properties of zeolite/N-doped porous carbon for the efficient removal of chemical oxygen demand and ammonia-nitrogen from aqueous solution, *RSC Adv.*, 2019, **1**, 6452–6459.

50 M. Gaouar, B. Benguella, N. Gaouar-Benyelles and K. Tizaoui, Adsorption of ammonia from wastewater using low-cost bentonite/chitosan beads, *Desalin. Water Treat.*, 2015, **3994**, 1–11.

51 R. Apiratikul and P. Pavasant, Sorption of $Cu^{2+}$, $Cd^{2+}$, and $Pb^{2+}$ using modified zeolite from coal fly ash, *Chem. Eng. J.*, 2008, **144**, 245–258.

52 L. Nthunya, *et al.*, Adsorption of phenolic compounds by polyacrylonitrile nanofibre membranes: A pretreatment for the removal of hydrophobic bearing compounds from water, *J. Environ. Chem. Eng.*, 2019, **7**, 103–254.

53 L. Lin, *et al.*, Adsorption mechanisms of high-levels of ammonium onto natural and NaCl-modified zeolites, *Sep. Purif. Technol.*, 2013, **103**, 15–20.

54 W. He, H. Gong, K. Fang, F. Peng and K. Wang, Revealing the effect of preparation parameters on zeolite adsorption performance for low and medium concentrations of ammonium, *J. Environ. Sci.*, 201, **85**, 177–188.